

Genetic structure of a European forest species, the edible dormouse (*Glis glis*): a consequence of past anthropogenic forest fragmentation?

J. R. MICHAUX^{1,2,*}, H. HÜRNER¹, B. KRYSSTUFEK³, M. SARÀ⁴, A. RIBAS⁵, T. RUCH⁶, V. VEKHNİK⁷ and S. RENAUD⁸

¹Conservation Genetics Laboratory, Institut de Botanique, Chemin de la Vallée, 4, 4000 Liège, Belgium

²CIRAD/INRA UMR117 ASTRE, Campus International de Baillarguet, 34398 Montpellier Cedex 5, France

³Slovenian Museum of Natural History, Presernova 20, SI-1000 Ljubljana, Slovenia

⁴Dipartimento STEBICEF, Via Archirafi, 18-90123 Palermo, Italy

⁵Museu de Granollers-Ciències Naturals C/ Francesc Macià, 51 08402 Granollers, Spain

⁶Institute for Cell Biology and Neuroscience, Johann Wolfgang-Goethe Universität Frankfurt am Main, AK NCR, Siesmayerstr. 70, D-60054 Frankfurt am Main, Germany

⁷445362 Zhiguli State Nature Reserve, Bakhilova Polyana Village, Samara Oblast, Russia

⁸Laboratoire de Biométrie et Biologie Evolutive, UMR 5558, Université Lyon 1, CNRS, 69622 Villeurbanne, France

Received 17 July 2018; revised 8 October 2018; accepted for publication 8 October 2018

The genetic structure of forest animal species may allow the spatial dynamics of the forests themselves to be tracked. Two scales of change are commonly discussed: changes in forest distribution during the Quaternary, due to glacial/interglacial cycles, and current fragmentation related to habitat destruction. However, anthropogenic changes in forest distribution may have started well before the Quaternary, causing fragmentation at an intermediate time scale that is seldom considered. To explore the relative role of these processes, the genetic structure of a forest species with narrow ecological preferences, the edible dormouse (*Glis glis*), was investigated in a set of samples covering a large part of its Palaearctic distribution. Strong and complex geographical structure was revealed from the use of microsatellite markers. This structure suggests that fragmentation occurred in several steps, progressively splitting the ancestral population into peripheral isolated ones. The fact that this structure postdates post-glacial recolonization, together with dating based on microsatellite data, supports the hypothesis that the differentiation was recent, starting around 9000 years ago, and took place stepwise, possibly up to Medieval times. This complements a classic phylogeographical interpretation based on the effect of past climate change, and supports the role of anthropogenic deforestation as a trigger of recent intraspecific differentiation.

ADDITIONAL KEYWORDS: ABC analysis – early anthropogenic deforestation – forest fragmentation – Gliridae – global change – phylogeography.

INTRODUCTION

Anthropogenic changes to the Earth's biosphere are now so great and so rapid that the concept of a new geological epoch, the Anthropocene, has been proposed. Its start is commonly attributed to the first increase of atmospheric CO₂ and CH₄ concentrations during the 1800s above previous long-term stable values, a view that emphasizes the role of recent anthropogenic changes related to industrialization. Yet, defined

by strong human impact on the environment, the Anthropocene might actually have started thousands of years ago (Ruddiman, 2003) as a result of the spread of agriculture and technological innovations in farming that resulted in massive deforestation in several areas (Fairservis, 1971; Hugues, 1975; Thirgood, 1981; Simmons, 1996).

The impact of humans on the natural fauna might thus be much older than is usually considered when

focusing on the effects of industrialization (Martin, 2005) and recent habitat destruction (although these actions are also of great concern because they are ongoing). There is increasing evidence that current habitat fragmentation is strongly affecting the genetic structure of animal populations (Gerlach & Musolf, 2000; Kyle & Strobeck, 2001; Wang & Schreiber, 2001; Hirota *et al.*, 2004; Keller *et al.*, 2004). In contrast, the potential impact of more ancient anthropogenic changes on the patterns of geographical differentiation of European wild species remains largely undocumented. The impact of deforestation (which encompasses habitat loss and fragmentation) can be assumed to be particularly strong for forest animals. Studies on such species could help to decipher the timing and processes relating animal differentiation to anthropogenic changes, although it is often difficult to distinguish between natural climate change and human-induced deforestation.

The edible dormouse (*Glis glis*) is a good candidate for such a study. Although occasionally gathering food in environments such as orchards (Carpaneto and Cristaldi, 1995), the species relies heavily on food and shelter in mature deciduous woodlands with mast-seeding trees such as beeches (*Fagus* spp.), oaks (*Quercus* spp.) and sweet chestnut (*Castanea sativa*) (Ruf *et al.*, 2006). It is a selective feeder, concentrating on the most nutritious food sources available (Holisova, 1968; Gigirey & Rey, 1999; Hürner & Michaux, 2009). These specific trophic requirements limit its occurrence to high-diversity environments that provide a continuity of adequate food supplies throughout the year. It may even skip reproduction in years of low food availability (Bieber & Ruf, 2009; Krystufek, 2010, Marteau & Sarà 2015). The edible dormouse is also a gregarious animal with large patch requirements and high habitat fidelity (see Krystufek, 2010). Together, these narrow ecological preferences make it highly sensitive to habitat fragmentation (Mortelliti *et al.*, 2008). Its large distribution area (Fig. 1), from the Baltic Sea in the north to the Mediterranean peninsulas (including Sicily) to the south, and from the Iberian region to the west to Russia and the Black Sea and Caspian coasts to the east (Krystufek, 2010), provides the opportunity to trace on a large geographical scale the potential impact of forest habitat structure on the evolutionary dynamics of the species.

Traditional phylogeographical interpretation would predict a differentiation during glacial/interglacial cycles, leading to the establishment of several main lineages in refuge areas, such as the Mediterranean peninsulas, more than 15 000 years ago. It is from these refuge areas that populations would have recolonized Northern Europe after the last glacial maximum (see Taberlet *et al.*, 1998; Hewitt, 1999; Michaux *et al.*, 2003, 2005; Boston *et al.*, 2015).

The phylogeographical structure of the edible dormouse has been assessed by analysis based on mitochondrial DNA (mtDNA) variation (Hürner *et al.*, 2010; Naderi *et al.*, 2014). This has revealed several endemic lineages at the southern fringe of its distribution, corresponding to refuge areas, and a recent post-glacial recolonization of most of Eurasia from a single Mediterranean refugium located in the Iberian region or in northern Italy. This led to a very low level of genetic diversity throughout most of the recolonized area. However, the use of detailed molecular markers such as microsatellites may reveal the existence of more recent events.

Using microsatellites on samples covering the whole distribution area of the edible dormouse (Fig. 1), we characterized its genetic structure with the aim to identify (1) whether finer genetic structure can be seen, post-dating the post-glacial recolonization traced by mitochondrial markers, and (2) the main drivers and the timing of such late differentiation (if any).

MATERIAL AND METHODS

SAMPLES AND DNA ANALYSIS

Tissue samples from 395 edible dormice from 47 sampling localities distributed throughout the geographical range of the species were analysed (Supporting Information, Table S1; Fig. 1). These specimens were obtained from collaborators, museums and our own fieldwork. In Belgium, where this species is protected by law, hair samples were collected non-invasively under the authorization of the Ministry of the Environment. All samples used were recent tissue specimens stored in ethanol except for the Hungarian samples which were dried hairs. DNA was isolated using the Qiagen DNeasy Tissue kit following the manufacturer's instructions. Samples were subject to genotyping at ten microsatellite loci using the multiplex sets defined by Hürner *et al.* (2009). PCR conditions were as reported by Hürner *et al.* (2009). Amplified DNA was analysed for length variations on an automated monocapillary ABI PRISM 310 Genetic Analyser (Applied Biosystems) using GENEMAPPER v.4.0 software (Applied Biosystems). To avoid rate errors, the dried hairs were analysed following the methods used for degraded DNA and the 'multitube' approach proposed by Taberlet *et al.* (1996), which requires that three positive PCRs are obtained for each locus and sample to be considered correct. MICRO-CHECKER 2.2.3 (Van Oosterhout *et al.*, 2004) was used to detect stutter errors and to estimate the proportion of null alleles at each locus. Genotypes were then corrected accordingly. This method revealed no error rates for the Hungarian samples. Tests for

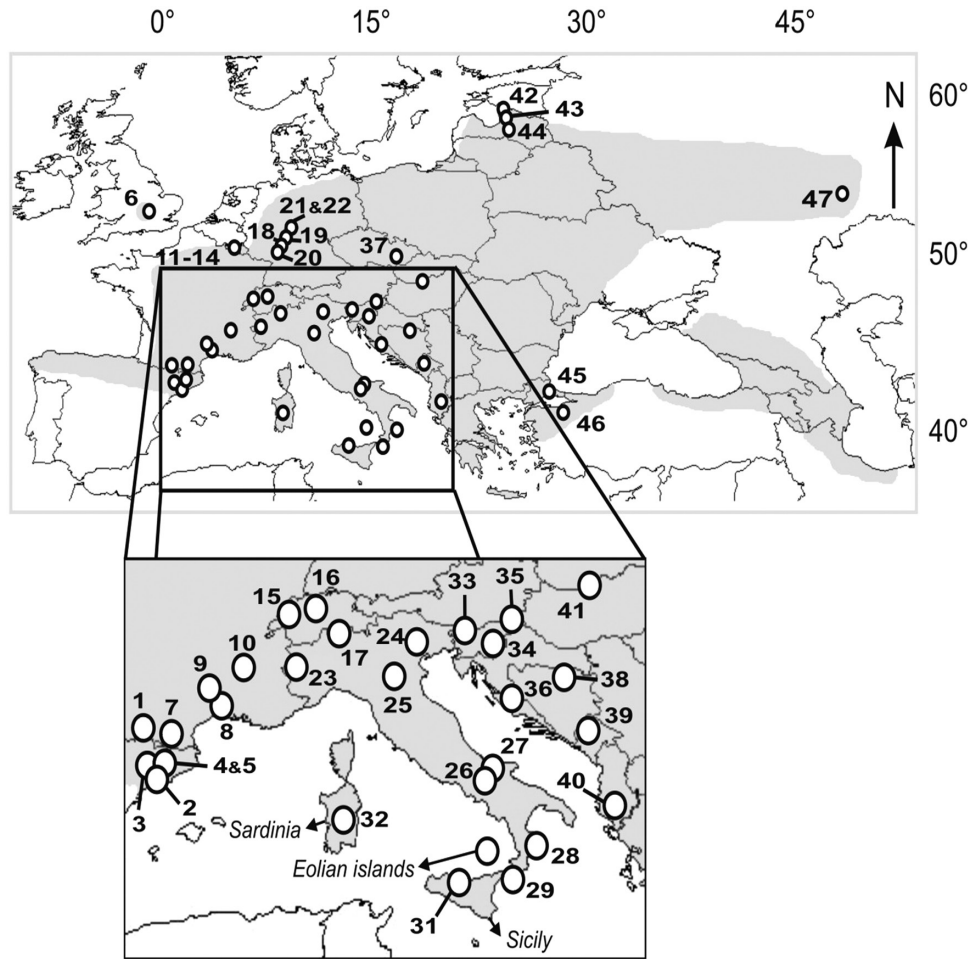


Figure 1. Map of sampling localities across the entire distribution range of the edible dormouse. Open circles: sampling localities (codes are given in Supporting Information, [Table S1](#)). The shaded zone corresponds to the distribution area of the species (after [Krystufek, 2010](#)).

linkage disequilibrium (10^4 permutations) were also performed using ARLEQUIN v.3.1, adjusting for multiple tests using sequential Bonferroni correction.

CLUSTER ANALYSIS

We applied two complementary Bayesian clustering algorithms, namely STRUCTURE v.2.3.3. ([Pritchard *et al.*, 2000](#)) and GENELAND v.4.0.3 ([Guillot *et al.*, 2012](#)), to infer population structure (i.e. the number of clusters, K) and to assign individuals to clusters probabilistically based on each multilocus genotype and, for GENELAND, on each spatial origin. These two approaches assume that populations are panmictic units with distinct allele frequencies.

The estimation procedure consisted of runs using trial values of the number of populations (K) and then comparing the estimated log probability of the data under each K . For STRUCTURE, we conducted

a series of independent runs with different proposals for K , testing all values from 1 to 15. Each run used 5×10^6 iterations after a burn-in of 5×10^5 , utilizing a model allowing for admixture and correlated allele frequencies. To ensure convergence of the Markov chain Monte Carlo (MCMC) procedure, we used ten replicates for each value of K and then checked the results visually for consistency. Generally, the number of distinct populations (K) is estimated from the model of K that maximizes the probability of the data, $\ln P(D)$, but for complex population structures a modal value of $\ln P(D)$ may not be apparent ([Rosenberg *et al.*, 2002](#)). In such instances, the value of K at the beginning of a 'plateau' of estimates of $\ln P(D)$ may be selected as this is the smallest value of K that captures the major structure in the data set ([Pritchard & Wen, 2003](#)). We also used the ΔK method ([Evanno *et al.*, 2005](#)) implemented with STRUCTURE HARVESTER ([Earl](#)

& vonHoldt, 2012) to find the most likely value of K present in the dataset.

The second algorithm, implemented in GENELAND 4.0.3, differs from that of Pritchard *et al.* (2000) mainly by explicitly taking into account the spatial dependence of individuals expected for a species whose range is much larger than the average inter-generation movement of individuals. This model assumes no admixture and aims to infer and locate genetic discontinuities between populations in space from individual geo-referenced multilocus genotypes, while taking into account uncertainty in the location of sampled individuals (Guillot *et al.*, 2012). All the parameters (including K) are co-estimated simultaneously by the MCMC algorithm. To optimize estimation of the parameters, a two-step procedure was applied: a first run to infer K and a second run with K fixed at the modal value to estimate the other parameters (mainly assignment of individuals to the inferred populations). The first step was replicated ten times to check for convergence, allowing K to vary from 1 to 15 clusters and using run parameters as follows: 10^6 MCMC iterations, maximum rate of Poisson process fixed at 700, maximum number of nuclei in the Poisson–Voronoi tessellation fixed at 500, and an uncertainty associated with the spatial coordinates of 1 km. We used the Dirichlet model of allelic frequencies as this has been demonstrated to perform better than the alternative model (Guillot *et al.*, 2005). We inferred the number of clusters (K) from the modal value of K for these ten runs, and then ran the MCMC procedure again 100 times with K fixed for this value, 1×10^6 MCMC iterations and the other modelling options unchanged. We calculated the mean logarithm of the posterior probability of the data (PPD) for each of the 100 runs and selected the ten runs with the highest PPD. These ten runs were then post-processed (with a burn-in of 3×10^4 iterations) to obtain posterior probabilities of population membership for each individual.

A visual output of the STRUCTURE and GENELAND results was generated using DISTRUCT (Rosenberg, 2004).

DIFFERENTIATION BETWEEN POPULATIONS

To determine the level of genetic differentiation at microsatellite loci, F_{st} (Weir & Cockerham, 1984) values among inferred clusters were calculated. A significance test was performed for F_{st} values after 10^4 permutations in ARLEQUIN v.3.1 (Excoffier *et al.*, 2005). To depict the overall relationship among all inferred clusters, we applied derived pairwise values of F_{st} to construct a neighbour-joining (NJ) tree with the program NEIGHBOUR in PHYLIP (Felsenstein, 2004). Moreover, to confirm the NJ tree obtained using F_{st}

values, we used the program POPULATIONS 1.2.31 (Langella, 1999) using different genetic distances, the D_a index (Nei *et al.*, 1983) and the standard genetic distance D_s index (Nei, 1987). Takezaki & Nei (2008) suggest using these indices when constructing phylogenetic trees from microsatellite data.

GENETIC DIVERSITY AMONG CLUSTERS AND BOTTLENECK ANALYSIS

Allelic richness (R_s) corrected for differences in sample size (fewer than ten samples), observed (H_o) and expected (H_e) heterozygosity and F_{is} values were calculated within each inferred cluster using FSTAT v.2.9.3 (Goudet, 2001). The significance of F_{is} values was assessed by comparing the observed values against distributions obtained by randomization (10^3 times) and adjusting for multiple tests using Bonferroni correction.

ISOLATION BY DISTANCE ANALYSES

Isolation by distance (IBD) among the identified clusters was tested by comparing pairwise geographical distance (log-transformed) with pairwise genetic distances, estimated as $F_{st}/(1 - F_{st})$ and $R_{st}/(1 - R_{st})$ using ARLEQUIN and SPAGeDI 1.3 (Hardy & Veekemans, 2002), respectively. IBD was calculated to assess whether genetic differentiation was distributed according to geographical distance.

TESTING ALTERNATIVE SCENARIOS BY ABC MODELLING

Approximate Bayesian computation (ABC) analyses are useful when investigating complex population genetics patterns based on microsatellite markers (e.g. Bryja *et al.*, 2010; Sunnåker *et al.*, 2013; Ali *et al.*, 2014; Olafsson *et al.*, 2014).

A set of different logical scenarios was therefore created (Supporting Information, Fig. S1) and tested using the ABC procedure (Beaumont *et al.*, 2002) in DIYABC v.2.0 (Cornuet *et al.*, 2008, 2014). This analysis allowed us to determine potential relationships among different clusters, which were then interpreted as populations (Fig. S1), and to estimate the timing of their differentiation.

To test alternative sequences of divergence of the different clusters, 17 scenarios were constructed. The first three were based on the topology obtained based on F_{st} values, and D_a and D_s genetic distances. The fourth scenario was constructed according to the progressive relationships among STRUCTURE clusters from the hypothesis of $K = 2$ to $K = 12$.

Thirteen further scenarios were built by rearrangement of branches with the 'Fst' scenario (as depicted in Fig. S1) used as a 'template', which was

modified according to the geographical proximity of the different populations as well as the biology of the species.

For each of these 17 scenarios, 5×10^5 datasets were simulated to build a reference table. To check if the combination of scenarios and previous distributions of their parameters was able to generate datasets similar to the one observed, a principal components analysis (PCA) was performed on the first 10 000 simulated datasets of the reference table in the space of summary statistics. The reference table was produced and recorded during the first step of ABC analyses. Each row of this table corresponds to a simulated dataset and contains the parameter values used to simulate the dataset and summary statistics computed based on the simulated dataset. Parameter values are drawn from previous distributions (Cornuet *et al.*, 2008). The summary statistics used were based on *F*_{st} values, mean numbers of alleles and mean genetic diversity. To determine the most likely scenario among the 17 tested scenarios, normalized Euclidean distances between each simulated dataset of the reference table and the observed dataset were then computed and the 1% closest simulated datasets were used to estimate the relative posterior probability (with 95% confidence intervals) of each scenario based on logistic regression. The most likely scenario had the highest posterior probability and non-overlapping 95% confidence intervals. Finally, the posterior density distributions of the effective population size of each population as well as the split times between them were estimated from the most likely scenario. Power analyses were used to evaluate the level of confidence.

We estimated type-I and type-II errors following Cornuet *et al.* (2010), by simulating 500 pseudo-observed datasets displaying properties similar to the observed dataset under the best scenario, and we computed the proportion of cases in which this scenario did not display the highest posterior probability. We estimated the false positive error rate (type-II error) by simulating 500 pseudo-observed datasets under each alternative scenario and computed the proportion of cases in which the scenario with the highest posterior probability was incorrectly selected as the most likely.

The prior distributions of parameters (effective population size, timing of events, chosen mutation model parameters for the microsatellites) used in the ABC analyses are summarized in Table S2. These parameters were chosen according to previous studies on *Glis* (Hürner *et al.*, 2010) as well as general mutation rates for microsatellite markers observed in rodents (Dietrich *et al.*, 1992). Broad intervals were chosen for each parameter, so that uncertainties in these parameters would not affect the output of the analysis. To estimate the timing of differentiation events, we considered one generation per year, as

generally considered for this species (Gazárková & Adamik, 2016).

MULTIVARIATE ANALYSIS OF MICROSATELLITE DATA

As an alternative means to visualize the relationships among populations, a multivariate analysis was performed on the microsatellite data. A principal coordinates analysis (PCoA) on microsatellite-based distances between individuals was used to extract synthetic axes explaining most of the total variation, without any a priori assumption regarding the structure of the data (Jombart *et al.*, 2009). The analysis was performed using the R package *ade4* (Dray & Dufour, 2007).

RESULTS

CLUSTERING ANALYSIS

Using STRUCTURE, the increase in likelihood when *K* (number of clusters) increases showed several important steps at *K* = 2, *K* = 5, *K* = 8 and *K* = 11 (ΔK method, Evanno *et al.*, 2005) (Fig. 2A). This suggests that the populations are hierarchically partitioned into several clusters of genetically similar populations. However, when considering the probability of successive partitions of the data when *K* increases (Fig. 2B), the estimated likelihood increases progressively and smoothly without reaching a clear plateau. This suggests a complex structure, although on this basis alone it is difficult to select a value of *K* capturing the major structure in the data, a problem exemplified by the fact that the assignments of the studied specimens when *K* was varied from 8 to 12 were often unclear (data not shown). The results of GENELAND, which considers the geographical locations of the samples, revealed a clearer picture. Indeed, posterior distributions of the estimated number of inferred clusters across ten replicates displayed a clear mode at *K* = 12 (Fig. 2C). The probability of membership of all specimens to these 12 clusters was obtained with DISTRUCT based on the highest-probability run (of ten) at that value of *K* (Fig. 3A). All individuals within each locality had a proportion of assignment to the inferred cluster of 100%, indicating that these results are robust. The geographical distribution of the mean probability per geographical area (Fig. 3B) showed that each cluster includes a set of geographically close populations. The 12 groups of populations corresponding to an individualized genetic cluster are: (1) North-Western Balkans (NWBa: Slovenia, north-eastern Italy, Croatia), (2) Belgium (BEL), (3) Italian peninsula (IT: north-western, central and southern Italy, Sardinia), (4) Balkans (BAL: Bosnia and

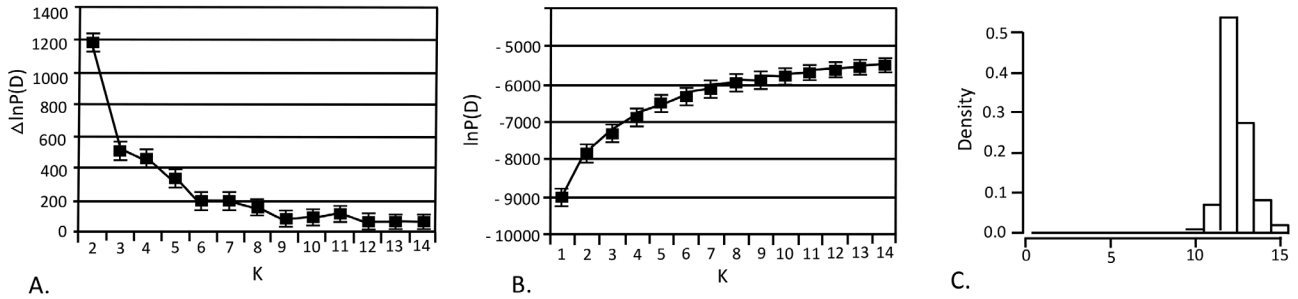


Figure 2. Estimation of the number of populations based on microsatellite data, analysed by STRUCTURE and GENELAND. A, differential variation of the probability of partitions into K and $K + 1$ clusters (Evanno *et al.*, 2005) obtained with STRUCTURE. Variation is calculated as $\Delta(\ln P(D) = \ln P(D)_{k+1} - \ln P(D)_k$. B, probability of successive partitions of the data into an increasing number of clusters obtained with STRUCTURE. Probability $[\ln P(D)]$ is estimated as the mean of ten replicated runs. For both A and B, the variance estimate is represented, which was calculated after five independent runs, using STRUCTURE HARVESTER. C, posterior distributions of the estimated number of inferred clusters across ten replicates obtained with GENELAND, displaying a clear mode at $K = 12$.

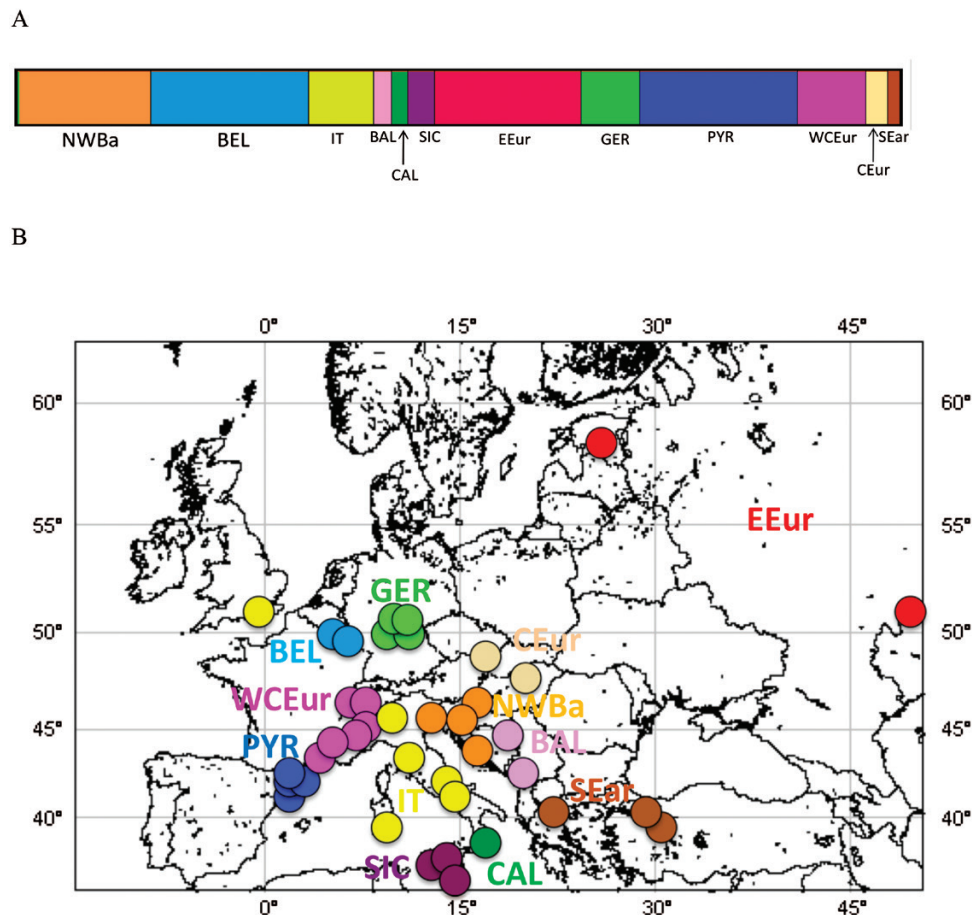


Figure 3. A, partitioning of the population structure of the edible dormouse for the modal solution $K = 12$, based on GENELAND analysis of the microsatellite data. Each individual is represented by a thin vertical line divided into K coloured segments representing the probability of membership of this individual to the K clusters. The different colours represent the different geographical groups emerging from the analysis. Individuals are arranged based on their country of origin and are sorted with increasing latitude. B, geographical representation of the outcomes for 12 genetic clusters ($K = 12$).

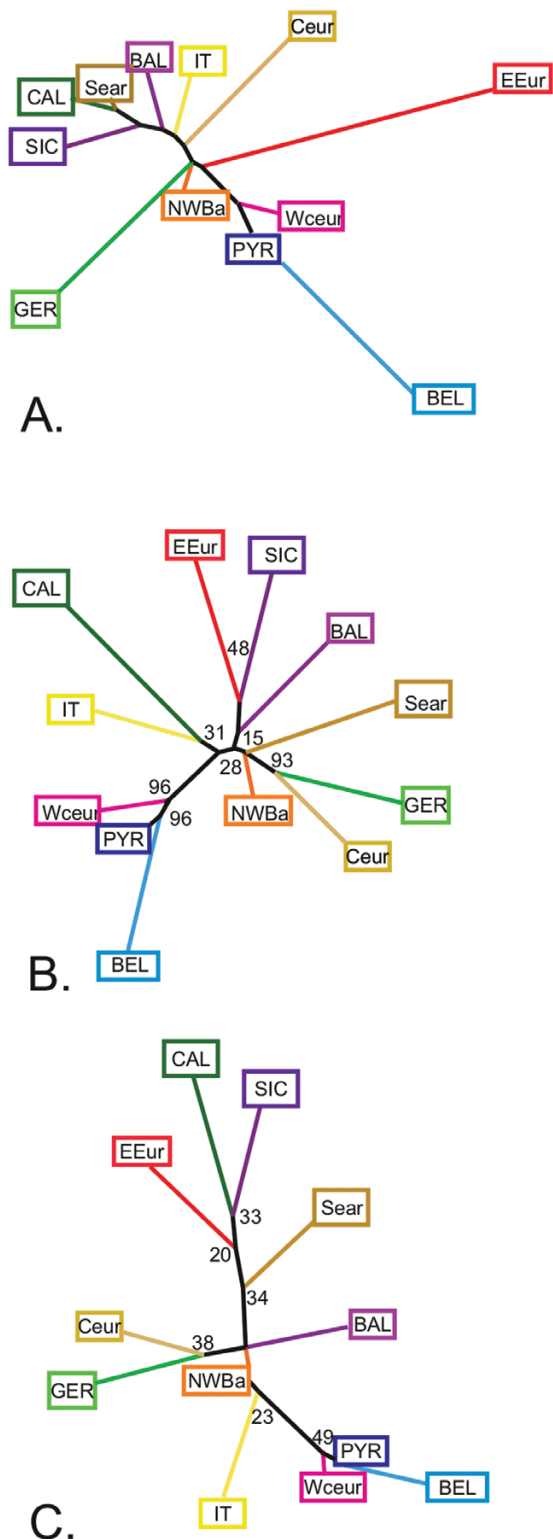


Figure 4. Phylogenetic relationships between the 12 genetic clusters of edible dormice, estimated by different phylogenetic methods. A, neighbour-joining tree based on pairwise F_{st} values. B, neighbour-joining tree using the D_a

Montenegro), (5) Southern Italy (CAL: Calabria), (6) Sicily and Aeolian Islands (SIC), (7) Eastern Europe (EEur: Russia and Latvia), (8) Germany (GER), (9) Northern Spain and French Pyrenees (PYR), (10) Western Central Europe (WCEur: south-east France/Switzerland), (11) Central Europe (CEur: Hungary, Czech Republic) and (12) South-Eastern areas (SEar: Turkey and Macedonia).

One exception to this geographical congruence emerged, between the genetically identified clusters and the sets of populations: the United Kingdom group (UK) appeared to be associated with the Italian peninsula group IT. This apparent geographical inconsistency is related to the recent artificial introduction of the edible dormouse to Great Britain. Hence, UK samples were not included in subsequent analyses.

DIFFERENTIATION BETWEEN POPULATIONS

Divergence between populations was estimated first by F_{st} values (Table S3). All pairwise F_{st} values were significantly different from zero, indicating that the clusters represented differentiated populations. The highest F_{st} values were recorded in pairwise comparisons involving northern peripheral populations: Russia/Latvia (EEur: mean F_{st} = 0.58), Belgium (BEL) (mean F_{st} = 0.56) and Germany (GER) (mean F_{st} = 0.45).

NJ analysis (Fig. 4A) based on F_{st} values provided an assessment of the hierarchical organization of the 12 clusters.

Different genetic groups were resolved. The first included populations from the Mediterranean area: Italian Peninsula (IT, CAL), Sicily (SIC), Balkans (BAL) and South Eastern areas (SEar). The Central European populations (CEur) appeared to be relatively closely related to this group. A set of populations clustered close together at the centre of the tree: North-Western Balkans (NWBa), Western Central Europe (WCEur) and Pyrenees (PYR). The remaining populations diverged from this central group of populations with longer branches: Belgium (BEL) branching close to Pyrenees (PYR) and Western Central Europe (WCEur) populations; Germany (GER) branching together with the North-Western Balkans (NWBa); and Eastern Europe (EEur) comprising a group on its own.

genetic distances index. C, neighbour-joining tree using the standard D_s genetic distance index. Colours are the same as in Figure 3. Values at the nodes in B and C correspond to bootstrap support values calculated with the program POPULATIONS.

The NJ trees obtained based on *Da* and *Ds* distances provided two further topologies, which showed many common features with the *Fst*-based pattern, but also some noticeable discrepancies. The tree based on *Da* distances (Fig. 4B) provided clearer support for the association of the westernmost populations (PYR, WCEur, BEL). On this basis, the Mediterranean cluster was split into two clades, one including only animals from the Italian Peninsula (IT and CAL) and the other including apparently disjoint populations (SIC, BAL and EEur). The German (GER) population was associated with the Central European one (CEur). NWBa again appeared close to the centre of the tree. Finally, the tree based on *Ds* distances (Fig. 4C) was quite similar to that obtained based on *Da* distances. The Western clade (WEur, PYR and BEL) again emerged and NWBa was close to the centre of the tree as in other topologies; GER was associated with CEur as seen based on *Ds* distances. Discrepancies were mostly found regarding Southern Europe, with some similarities to the *Fst* tree and others to the *Dst* tree. IT and BAL appeared isolated but branched close to the North Western Balkan (NWBa) population. CAL, SIC, EEur and SEar clustered within a clade corresponding to the Southern and Eastern fringe of the geographical range. However, bootstrap values characterizing these last nodes were low and the difference among the trees should be taken with caution.

ISOLATION BY DISTANCE

IBD was not detected among the 12 populations using both *Fst* and *Rst* values ($R^2 = 0.11$, $P = 0.36$; and $R^2 = 0.10$, $P = 0.29$, respectively). This suggests that despite the geographical coherence of the clusters of populations, the genetic structure observed in our dataset cannot be explained merely by geographical distance, but rather corresponds to patches of interconnected populations isolated from each other.

GENETIC DIVERSITY WITHIN POPULATIONS

Expected and observed heterozygosity and *Fis* values were estimated for all populations except Sardinia, which was too poorly sampled ($N = 2$, Table S1). The majority of the sampled populations conformed to Hardy–Weinberg (HW) equilibrium at most of the loci after sequential Bonferroni correction. The locus/population combinations that were not in HW equilibrium (heterozygote deficiency) were not specific to a particular population or locus. We therefore decided to maintain all of the loci in further analyses. There was no evidence of linkage disequilibrium after Bonferroni correction. These results confirm that our dataset is compatible with the clustering approach, the assumptions of which require that clusters are

sampled from discrete genetic units at HW and linkage equilibrium.

Mean allelic richness (*Rs*) ranged from 1.8 for BEL to 6 for SIC (Table 1). Average observed heterozygosity within populations varied from 0.14 to 0.63 and expected heterozygosity within populations from 0.18 to 0.75 (Table 1).

MULTIVARIATE ANALYSIS OF THE MICROSATELLITE DATA

Peripheral populations (BEL, GER and EEur) appeared to be the most divergent on the two principal axes of the PCoA, in total representing more than 38% of the variance (Fig. 5). Furthermore, along the first axis, a gradient emerged contrasting the western (PYR, WCEur and BEL) and eastern groups (EEur as the most extreme; SEar, CAL, SIC and, to a lesser extent, BAL). Geographically intermediate locations were also intermediate along the first PCoA axis (IT close to the UK, CEur and NWBa populations). Overall, the structure that emerged was similar to those retrieved from *Fst*, *Da* and *Ds* distances, but there was differentiation of peripheral populations.

POPULATION HISTORY INFERRED BY ABC ANALYSIS

The Bayesian approach allowed us to make inferences regarding the reconstruction of population history based on several steps. First, a PCA performed on the first 10 000 simulated datasets of the reference table in the space of summary statistics revealed that the observed dataset was encompassed by simulated datasets, indicating that our model was able to produce datasets similar to the one observed

Table 1. Estimates of multilocus genetic variation for all groups comprising five or more individuals

Group	<i>N</i>	<i>Rs</i>	<i>Ho</i>	<i>He</i>	<i>Fis</i>
BEL	70	1.8	0.18	0.18	0.199
PYR	70	3.6	0.37	0.51	0.283
WCEur	30	3.4	0.45	0.51	0.111
GER	26	2.6	0.23	0.33	0.367
EEur	65	2.2	0.14	0.19	0.255
CEur	10	3.7	0.43	0.56	0.234
CAL	7	5.1	0.51	0.64	0.304
BAL	8	3.6	0.40	0.42	0.059
UK	11	3.4	0.56	0.57	0.122
NWBa	59	3.6	0.41	0.45	0.165
SEar	5	2.0	0.26	0.27	0.012
SIC	19	6.0	0.48	0.75	0.358

N, number of specimens per group; *Rs*, allelic richness corrected for sample size; *Ho*, observed heterozygosity; *He*, expected heterozygosity; *Fis*, inbreeding coefficient.

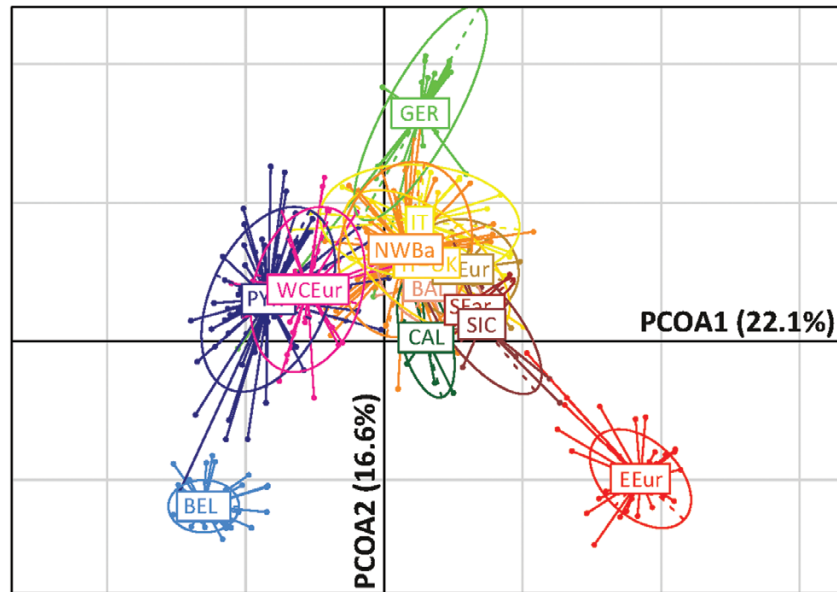


Figure 5. Between-group dispersion of the microsatellite data, represented on the first two axes of a PCoA. Ellipses summarize the variation within each of the geographical groups of edible dormice (based on GENELAND analysis, $K = 12$). The colour code is as for Figures 3 and 4.

(Fig. S2). The final step of our Bayesian approach was a set of logistic regressions, which were performed on the closest 1% of the simulated datasets. This allowed us to unambiguously distinguish the most likely of the tested scenarios. The observed topology based on D_s distances (i.e. scenario 3 in Fig. 4C) was statistically the most robust, supported by posterior probabilities three times higher than the second ranked scenario, based on D_a distances (D_s -based topology: $P = 0.579 \pm 0.322$ – 0.669 vs. D_a -based topology: $P = 0.212 \pm 0.197$ – 0.265) whereas all other topologies had a P -value < 0.05 . (Supporting Information, Fig. S3). Power analyses based on test datasets simulated under the 17 scenarios indicated that, given the size and polymorphism of the dataset, the method has high power to distinguish between the competing scenarios tested. More precisely, we estimated the performance of the analysis: of the thousands of pseudo-observed datasets generated using scenario 3, 46.4% were correctly identified as having been generated under this model. A moderate proportion (10.2%) were incorrectly attributed under scenario 2. The type-II error rate was low for the datasets generated under most scenarios (Table S4).

These results provide estimates of the periods of differentiation (Table S5) that would have led to the present genetic structure of the edible dormouse (Fig. 6A). Although these estimates should be considered with caution given that the population of origin may not have been panmictic, as postulated

in our analyses, they do suggest four successive periods of differentiation, all clearly after the last Ice Age, which corroborates the results obtained with mtDNA (Hürner *et al.*, 2010). These periods are:

- (1) an initial step of differentiation, at the beginning of the Holocene (around 9000 years ago), separating four ancestral stocks approximately corresponding to South and East Europe, Balkans, Northern Central Europe, and Central to Western Europe (Fig. 6B);
- (2) a succeeding split of these ancestral stocks between 6000 and 7000 years ago, especially affecting North Western Balkans (NWBa) and Eastern areas;
- (3) a third phase of differentiation during the Neolithic (between 5000 and 4000 years ago), which drove the separation among (i) populations from Calabria (CAL) and Sicily (SIC), (ii) populations from Germany (GER) and Central Europe (CEur), and (iii) populations from continental Italy (IT) and the Western European clade; and
- (4) finally the last period of differentiation during Medieval times (between the 5th and 11th centuries AD), driving the separation of the Western European group [Belgium (BEL), Pyrenees (PYR), West Central Europe (WCEur)].

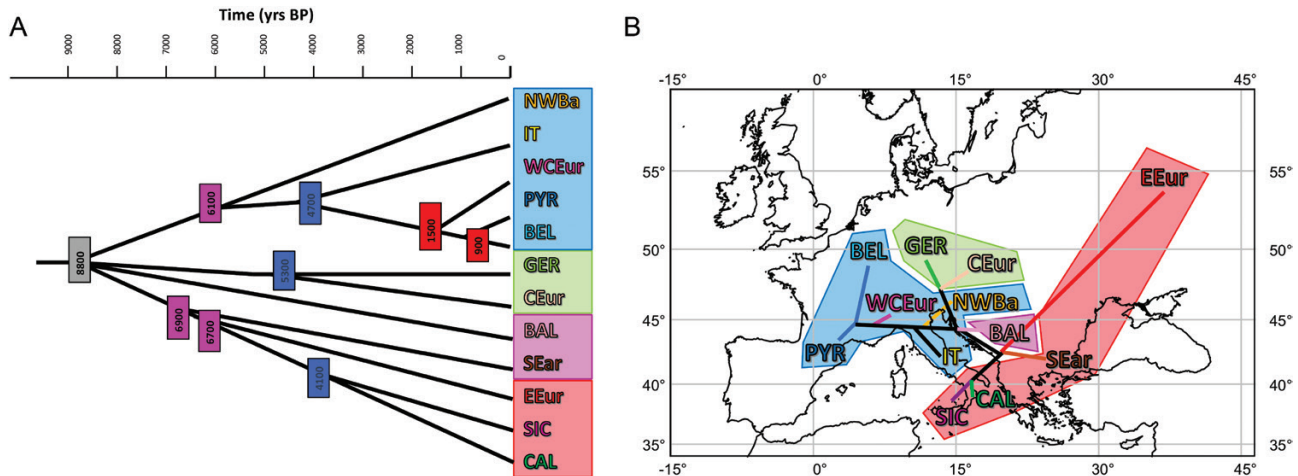


Figure 6. A, representation of the best scenario corresponding to the neighbour-joining (NJ) tree obtained with Ds values and validated using ABC analyses. Split times corresponding to the mean values of the posterior probabilities (see Table 2) are given at each node. The grey colour corresponds to the first period of diversification (8500–9000 years BP), pink to the second one (6000–7000 years BP), blue to the third one (4000–5000 years BP) and red to the last period of differentiation (900–1500 years BP). B, representation on a European map of the best scenario of splitting events between populations (corresponding to the NJ tree based on Ds values). The four main genetic groups, which differentiated during the first period of diversification (8500–9000 years BP), are represented as shaded rectangles in A and shaded polygons with the same colours in B. The names of the studied populations are also given (BEL, PYR, WCEur, GER, EEur, NWBa, CEur, IT, CAL, SIC, EEur, BAL). Colours are as for Figures 3 and 4.

DISCUSSION

The present study represents the most thorough research on the population genetics of the edible dormouse. Previous analyses based on mtDNA (Hürner *et al.*, 2010; Naderi *et al.*, 2014) have shown a Europe-wide genetic homogeneity for the species, except at the southern fringe of its distribution (Italian peninsula, Sicily, the Balkans, the Middle East, Iran), locations characterized by a slightly higher genetic diversity and which perhaps acted as refuges for this species. Results suggest that Quaternary glaciations led to the differentiation of multiple lineages within this species, as in other rodents such as the hazel dormouse (*Muscardinus avellanarius*; Mouton *et al.*, 2012, 2016), woodmice (Michaux *et al.*, 2003, 2005; Herman *et al.*, 2017) and bank voles (Deffontaine *et al.*, 2005; Filipi *et al.*, 2015), but that only lineage contributed to the post-glacial recolonization of the rest of Europe.

Microsatellite markers, having a higher evolutionary rate than mtDNA, have the potential to provide evidence of more recent and precise diversification events. Indeed, beyond the genetic homogeneity within the edible dormouse in most of Europe shown by mtDNA analysis, the present analysis revealed a recent complex evolutionary history. Even allowing for the methodological limits for the estimates of divergence time, the microsatellite results support the hypothesis that the basal divergence between

the Western, Central and Eastern European groups occurred well after the last glacial maximum (22 000–15 000 years BP) (Fig. 6A; Table 2). Accordingly, we propose the following scenario of genetic differentiation of the edible dormouse populations in Europe. First, an initial split of the main lineages took place during the mid-Holocene (between 9000 and 8000 years BP); second, differentiation in the South-Eastern region between 7000 and 6000 years ago; third a further split in different regions of Europe, including Central and South-Western Europe, occurring between 5000 and 4000 years ago; and finally, a phase of local divergence within Western European regions as late as Medieval times (1500–900 years BP).

The edible dormouse is a thermophilous rodent that is highly dependent on mature deciduous woodlands. As such, it was presumably severely affected by the climatic fluctuations of the Quaternary that drove it from its preferred habitat into a few refugia, namely the classic European refuge areas (Sommer & Nadachowski, 2006) – Iberia, Italian peninsula, the Balkans and the Hyrcanian region – and led to the differentiation of mtDNA lineages (Hürner *et al.*, 2010; Naderi *et al.*, 2014). These southern lineages, however, did not contribute to the recolonization of most of Europe or even Eurasia. Rather, recolonization occurred from a single refuge in the Iberian region or northern Italy, where most mtDNA diversity occurs

today and where those haplotypes characterizing all northern European populations (mtDNA lineage 3) are present (Hürner *et al.*, 2010). In agreement with this, fossil evidence of edible dormice has been recorded in the Iberian Peninsula for the last glacial maximum (Sommer & Nadachowski, 2006). The edible dormouse shows low dispersal and is specialist feeder that is strongly adapted to temperate forests and is temporally and spatially dependent on seed-mast crops (Bieber, 1998; Scinski & Borowski, 2008; Bieber & Ruf, 2009). This specialization may have made it prone to random extinction in an unstable environment such as that of northern Europe at the end of the last glacial maximum, explaining its absence during the coldest periods from almost all regions (Sommer and Nadachowski, 2006).

The timing of differentiation (between 9000 and 4000 years BP) between the southern groups (IT, CAL, BAL, NWBa) based on microsatellite data, as well as their very weak genetic differentiation based on microsatellite markers (see PCoA), however, contradicts with the persistence in these areas of mtDNA genetic lineages inherited during glacial/interglacial cycles (Hürner *et al.*, 2010).

While the haploid nature and uniparental transmission of mtDNA can contribute to stronger genetic drift at local or regional geographical scales, these results could also be explained in part by female philopatry (Weber *et al.*, 2018) and male-mediated dispersal. Indeed, this can explain the strong structure of female-linked markers, while differentiation of biparentally transmitted loci is homogenized by male-mediated gene flow (Fahey *et al.*, 2014). Therefore, genetic exchange might have occurred among the southern populations soon after the last glacial maximum, blurring the signal of glacial/interglacial structure at the nuclear level, but still maintaining the high mtDNA genetic structure observed in these populations, especially given that mtDNA markers evolve much more slowly than microsatellites. Hence, despite the high F_{st} values, the observed interpopulation differentiation is quite recent.

CURRENT GENETIC STRUCTURE OF THE EDIBLE DORMOUSE: A CONSEQUENCE OF EARLY HUMAN DEFORESTATION?

A striking feature emerging from our results is that all phases of fragmentation between populations of the edible dormouse clearly postdated the last ice age, ranging up to the mid-Holocene and Medieval times. This agrees with the Europe-wide homogeneity evidenced by more slowly evolving markers (mtDNA), which suggest range expansion after the last glacial maximum (Hürner *et al.*, 2010). The relative effects of climate change and human impact on vegetation during the Holocene are difficult to disentangle (Jalut

et al., 2009; Marquer *et al.*, 2017). Climate might have been the primary driver of vegetation changes at the beginning of the Holocene (Jalut *et al.*, 2009; Marquer *et al.*, 2017), but later, human impact progressively increased (Roberts *et al.*, 2018).

Hence, climate change might at first have favoured an expanded range of the edible dormouse, since the area of forest in Europe was at a maximum during the mid-Holocene thermal optimum (Roberts *et al.*, 2018). Thereafter, the effects of climate change and human activity became intermingled, with increasing human impacts during the Late Holocene (Marquer *et al.*, 2017; Roberts *et al.*, 2018). In particular, the phases of population splits occurring after ~5000 years BP correspond roughly to periods when land use became a major driver of vegetation change (Marquer *et al.*, 2017). Because deciduous forests, the preferred habitat of the edible dormouse, were often associated with land that was suitable for conversion to agriculture (Roberts *et al.*, 2018), they were especially impacted by this increase in human land use.

Human impacts on the distribution of forest occurred in different phases. The Neolithic in Europe, corresponding to the transition from hunter-gatherers to the first farmers, spread from the Near East into south-eastern Europe as early as ~9500 years BP and progressed northward and westward along the Mediterranean coast and across the continent (Danubian stream), a process completed on the continent by 7500–7000 years BP (Zohary & Hopf, 1993; Tresset & Vigne 2011). Splits among edible dormouse populations started around 9000 years BP in south-east Europe, progressing thereafter westward and northward, and these were more complex in areas such as the Balkans, which were affected early during the Neolithic. Overall, this suggests that the isolation of different populations of edible dormice and their progressive genetic differentiation might have been due to a combination of climate change, especially for the early differentiation events, and increasing human impact on the landscape, starting soon after the Neolithic switch to farming practices.

The latest phase of differentiation, corresponding to a split of Western European populations, seems to have occurred during Medieval times, a period known for intense deforestation related to monastic activity (Gimpel, 1976; Dubois, 1989; Bechmann, 1990). Together, the divergence time estimates suggest that early anthropogenic impact might have severely affected the distribution of the edible dormouse. This is corroborated by fossil records for Iberia, which show continuous occupation after its recolonization following the last glacial maximum, but its disappearance as a result of anthropogenic change during the Bronze Age, ~3000 years ago (Cuenca-Bescos *et al.*, 2009). A similarly recent structuring of populations of edible dormice has

been suggested to have occurred along the Black Sea coast in relation to partly anthropogenic fragmentation of forest habitats (Helvacı *et al.*, 2012).

If confirmed, this dynamic population differentiation linked to forest fragmentation is probably ongoing, as shown by the congruence between the distribution of population clusters of the edible dormouse and areas with remnant patches of primary forests in Europe (Sabatini *et al.*, 2018). The rarity of such preserved habitats may contribute strongly to the rarity of the edible dormouse in the northern part of its distribution, where it is of conservation concern. Three effects may have contributed to the low genetic diversity in these remaining populations: low initial diversity related to post-glacial recolonization from a single source population in peripheral environments; a location at the leading edge of the expansion, which may also explain the lower genetic diversity compared to other populations; and the creation of forest fragments that probably shrank over time in highly populated areas such as Belgium and Germany. Restricted gene flow between populations possibly promoted genetic drift and led to high genetic differentiation among populations (previously unsuspected). However, this fragmentation increased inbreeding, with an associated loss of genetic diversity, reducing the capacity of small, isolated populations to adapt to environmental change (Saccheri *et al.*, 1998; Frankham *et al.*, 2002).

ISLANDS: SINK OR HOTSPOTS OF DIVERSITY?

Insular populations would appear to be particularly sensitive to extinction and, hence, to be less likely than continental counterparts to survive in the long term, as their genetic diversity is generally lower (Frankham, 1997). Nevertheless, two insular populations included here (Sicily and Great Britain) displayed surprisingly high genetic diversity (Table 1), suggesting unique evolutionary histories for these populations of dormice. The role of human activities is clear for the English population, which comprises specimens that were deliberately introduced at the beginning of the 20th century (Morris, 1997). In contrast to previous hypotheses, which suggested the origin of this population in Central Europe (Hungary, Germany or Switzerland) (Harris & Yalden, 2008), our results suggest strongly that the origin of these animals is continental Italy. As this last region is considered the main glacial refugium for the species and as it is characterized by having a high level of genetic diversity, it is not surprising that the British population also appears to be genetically diverse.

In Sicily, a high level of genetic diversity is preserved in various species of mammals, and more generally among vertebrates and invertebrates, despite its isolation from the continent (e.g. Michaux *et al.*, 1998,

2003; Nieberding *et al.*, 2006; Stöck *et al.*, 2008). This unique phylogeographical history is related to the Mediterranean Sea, which (1) buffered the impact of the last ice age and allowed the island to play a role as a refugium during the last ice age, and (2) impeded the invasion of many competitors and predators to the island (Michaux *et al.*, 2002). Moreover, for a small rodent like the edible dormouse, the large area of Sicily would be enough to sustain important population sizes and maintain a high level of genetic diversity.

CONCLUSION

The significant role of early human activity on wild fauna has long been appreciated, especially with regard to extinctions of emblematic species such as those belonging to the Pleistocene megafauna (Alroy, 2001; Roberts *et al.*, 2001), but also extinctions of less emblematic taxa of small rodents (Vigne & Valladas, 1996), and even microevolutionary adaptive processes in response to anthropogenic environmental perturbations (Bochaton *et al.*, 2017). The present study further suggests a discrete but decisive early anthropogenic impact on modern faunas, namely of early human-driven deforestation on the genetic structure of a forest species. Increasing evidence indicates that humans strongly impacted their environment much earlier than currently accepted, being responsible in the early Holocene for an increased greenhouse effect (see Ruddiman, 2003, 2007, 2011) and for distinct landscape modifications (Kaplan *et al.*, 2010; Klein Goldewijk *et al.*, 2010). The present study suggests another aspect of this ancient anthropogenic impact on wildlife, namely profound changes in the population structure of some mammals, such as the edible dormouse. How this species will be affected by current environmental change remains of debate. Our results emphasize that conservation measures for this species should target connections between areas of deciduous forest to limit the impact of forest fragmentation. However, the edible dormouse may benefit from modern social, political and agricultural trends that are favouring the reforestation of European landscapes (Moreira & Russo, 2007; Sitzia *et al.*, 2010; Garcia-Feced *et al.*, 2011).

ACKNOWLEDGMENTS

We are grateful to Alec de Selliers de Moreville for financial support that enabled the creation of the bank of microsatellites. We are grateful to the many people who assisted with this study by providing edible dormouse samples from throughout Europe: P. Adamik, A. Arrizabalaga, S. Bertolino, P. Gauberville, R. Libois, P. Morris and P. Vogel as well as P. Chevrete

for numerous discussions. H.H. was supported by a Belgian research fellowship from the FRIA (Fonds pour la Formation et la Recherche dans l'Industrie et dans l'Agriculture) and J.R.M. from the FNRS (Mandat 'Directeur de Recherches', Fonds National pour la Recherche Scientifique) and financial grants of the Belgian FNRS (crédits aux chercheurs to J.R.M.), and M.S. from the project supported by the Italian Ministry of Education, University and Research: PRIN 2010/2011 - 20108TZKHC "Climate change and animal populations: predictive models for mammals and birds". V.A. Vekhnik was funded by a regional grant of the Russian Foundation for Basic Research for Samara oblast according to the research project N 17-44-630288. B.K. acknowledges financial support from the Slovenian Research Agency (research core funding no. P1-0255).

REFERENCES

- Ali S, Gladieux P, Leconte M, Gautier A, Justesen AF, Hovmøller MS, Enjalbert J, de Vallavieille-Pope C. 2014. Origin, migration routes and worldwide population genetic structure of the wheat yellow rust pathogen *Puccinia striiformis* f.sp. *tritici*. *PLoS One* **10**: e1003903.
- Alroy J. 2001. A multispecies overkill simulation of the end-Pleistocene megafaunal mass extinction. *Science* **292**: 1893–1896.
- Beaumont MA, Zhang W, Balding DJ. 2002. Approximate Bayesian computation in population genetics. *Genetics* **162**: 2025–2035.
- Bechmann R. 1990. *Trees and man: the forest in the middle ages*. New York: Paragon House.
- Bieber C. 1998. Population dynamics, sexual activity, and reproduction failure in the fat dormouse (*Myoxus glis*). *Journal of Zoology* **244**: 223–229.
- Bieber C, Ruf T. 2009. Habitat differences affect life history tactics of a pulsed resource consumer, the edible dormouse (*Glis glis*). *Population Ecology* **51**: 481–492.
- Bochaton C, Bailon S, Herrel A, Grouard S, Ineich I, Tresset A, Cornette A. 2017. Human impacts reduce morphological diversity in an insular species of lizard. *Proceedings of the Royal Society B: Biological Sciences* **284**: 20170921.
- Boston ESM, Montgomery I, Hynes WR, Prodöhl PA. 2015. New insights on postglacial colonization in western Europe: the phylogeography of the Leisler's bat (*Nyctalus leisleri*). *Proceedings of the Royal Society B: Biological Sciences* **282**: 20142605.
- Bryja J, Smith C, Konečný A, Reichard M. 2010. Range-wide population genetic structure of the European bitterling (*Rhodeus amarus*) based on microsatellite and mitochondrial DNA analysis. *Molecular Ecology* **19**: 4708–4722.
- Carpaneto GM, Cristaldi M. 1995. Dormice and man: a review of past and present relations. *Hystrix* **6**: 303–330.
- Cornuet JM, Pudlo P, Veyssier J, Dehne-Garcia A, Gautier M, Leblois R, Marin JM, Estoup A. 2014. DIYABC v2.0: a software to make approximate Bayesian computation inferences about population history using single nucleotide polymorphism, DNA sequence and microsatellite data. *Bioinformatics* **30**: 1187–1189.
- Cornuet JM, Ravigné V, Estoup A. 2010. Inference on population history and model checking using DNA sequence and microsatellite data with the software DIYABC (v1.0). *BMC Bioinformatics* **11**: 401.
- Cornuet JM, Santos F, Beaumont MA, Robert CP, Marin JM, Balding DJ, Guillemaud T, Estoup A. 2008. Inferring population history with DIY ABC: a user-friendly approach to approximate Bayesian computation. *Bioinformatics* **24**: 2713–2719.
- Cuenca-Bescos G, Straus LG, Moralez MRG. 2009. The reconstruction of past environments through small mammals: from the Mousterian to the Bronze Age in El Miron Cave (Cantabria, Spain). *Journal of Archaeological Science* **36**: 947–955.
- Deffontaine V, Libois R, Kotlík P, Sommer R, Nieberding C, Paradis E, Searle JB, Michaux JR. 2005. Beyond the Mediterranean peninsulas: evidence of central European glacial refugia for a temperate forest mammal species, the bank vole (*Clethrionomys glareolus*). *Molecular Ecology* **14**: 1727–1739.
- Dietrich W, Katz H, Lincoln SE, Shin HS, Friedman J, Dracopoli NC, Lander ES. 1992. A genetic map of the mouse suitable for typing intraspecific crosses. *Genetics* **131**: 423–447.
- Dray S, Dufour AB. 2007. The ade4 package: implementing the duality diagram for ecologists. *Journal of Statistical Software* **22**: 1–20.
- Dubois JJ. 1989. *Espaces et milieux forestiers dans le Nord de la France. Vol. 2. Étude de biogéographie historique*. Thèse d'État, Université Paris-I Panthéon-Sorbonne.
- Earl DA, vonHoldt BM. 2012. Structure Harvester: a website and program for visualizing STRUCTURE output and implementing the Evanno method. *Conservation Genetics Research* **4**: 359–361.
- Evanno G, Regnaut S, Goudet J. 2005. Detecting the number of clusters of individuals using the software STRUCTURE: a simulation study. *Molecular Ecology* **14**: 2611–2620.
- Excoffier L, Laval G, Schneider S. 2005. Arlequin (version 3.0): an integrated software package for population genetics data analysis. *Evolutionary Bioinformatics Online* **1**: 47–50.
- Fahey AL, Ricklefs RE, Dewoody JA. 2014. DNA-based approaches for evaluating historical demography in terrestrial vertebrates. *Biological Journal of the Linnean Society* **112**: 367–386.
- Fairservis WA Jr. 1971. *The roots of ancient India*. New York: MacMillan.
- Felsenstein J. 2004. *PHYLIP (Phylogeny inference package), Version 3.6*. Available at: <http://evolution.genetics.washington.edu/phylip.html>.
- Filipi K, Marková S, Searle JB, Kotlík P. 2015. Mitogenomic phylogenetics of the bank vole *Clethrionomys glareolus*, a model system for studying end-glacial colonization of Europe. *Molecular Phylogenetics and Evolution* **82**: 245–257.
- Frankham R. 1997. Do island populations have less genetic variation than mainland populations? *Heredity* **78**: 311–327.

- Frankham R, Ballou JD, Briscoe DA. 2002.** *Introduction to conservation genetics*. New York: Cambridge University Press.
- García-Feced C, Saura S, Elena-Rossello R. 2011.** Improving landscape connectivity in forest districts: a two-stage process for prioritizing agricultural patches for restoration. *Forest Ecology and Management* **261**: 154–161.
- Gazárková AH, Adamik P. 2016.** Timing of breeding and second litters in edible dormouse (*Glis glis*). *Folia Zoologica* **65**: 165–168.
- Gerlach G, Musolf K. 2000.** Fragmentation of landscape as a cause for genetic subdivision in bank voles. *Conservation Biology* **14**: 1066–1074.
- Gigirey A, Rey JM. 1999.** Faecal analysis of the edible dormouse (*Glis glis*) in the northwest Iberian Peninsula. *Zeitschrift für Säugetierkunde* **64**: 376–379.
- Gimpel J. 1976.** *The medieval machine: the industrial revolution of the middle ages*. New York: Penguin Books.
- Goudet J. 2001.** *FSTAT: a program to estimate and test gene diversities and fixation indices (version 2.9.3)*. Available at: <http://www2.unil.ch/popgen/softwares/Fstat.htm>.
- Guillot G, Estoup A, Mortier F, Cosson JF. 2005.** A spatial statistical model for landscape genetics. *Genetics* **170**: 1261–1280.
- Guillot G, Renaud S, Ledevin R, Michaux J, Claude J. 2012.** A unifying model for the analysis of phenotypic, genetic, and geographic data. *Systematic Biology* **61**: 897–911.
- Hardy OJ, Vekemans X. 2002.** SPAGeDi: a versatile computer program to analyse spatial genetic structure at the individual or population levels. *Molecular Ecology Notes* **2**: 618–620.
- Harris S, Yalden DW. 2008.** *Mammals of the British Isles: handbook, 4th edn*. Southampton: The Mammal Society.
- Helvacı Z, Renaud S, Ledevin R, Adriaens D, Michaux JR, Çolak R, Kankiliç T, Kandemir I, Yiğit N, Çolak E. 2012.** Morphometric and genetic structure of the edible dormouse (*Glis glis*): a consequence of forest fragmentation in Turkey. *Biological Journal of the Linnean Society* **107**: 611–623.
- Herman JS, Jóhannesdóttir F, Jones EP, McDevitt AD, Michaux JR, White TA, Wójcik JM, Searle JB. 2017.** Post-glacial colonization of Europe by the wood mouse, *Apodemus sylvaticus*: evidence of a northern refugium and dispersal with humans. *Biological Journal of the Linnean Society* **120**: 313–332.
- Hewitt GM. 1999.** Post-glacial re-colonization of European biota. *Biological Journal of the Linnean Society* **68**: 87–112.
- Hirota T, Hirohata T, Mashima H, Satoh T, Obara Y. 2004.** Population structure of the large Japanese field mouse, *Apodemus speciosus* (Rodentia: Muridae), in suburban landscape, based on mitochondrial D-loop sequences. *Molecular Ecology* **13**: 3275–3282.
- Holisova V. 1968.** Notes on the food of edible dormice (Gliridae). *Zoologické Listy* **17**: 109–114.
- Hugues JD. 1975.** *Ecology in ancient civilizations*. Albuquerque: University of New Mexico Press.
- Hürner H, Krystufek B, Sarà M, Ribas A, Ruch T, Sommer R, Ivashkina V, Michaux JR. 2010.** Mitochondrial phylogeography of the edible dormouse (*Glis glis*) in the Western palaeartic region. *Journal of Mammalogy* **91**: 233–242.
- Hürner H, Martin JF, Ribas A, Arrizabalaga A, Michaux JR. 2009.** Isolation, characterization and PCR multiplexing of polymorphic microsatellite markers in the edible dormouse, *Glis glis*. *Molecular Ecology Resources* **9**: 885–887.
- Hürner H, Michaux JR. 2009.** Ecology of the edible dormouse (*Glis glis*) in a Western edge population in Southern Belgium. *Vie et Milieu* **59**: 243–250.
- Jalut G, Deboudat JJ, Fontugne M, Otto T. 2009.** Holocene circum-Mediterranean vegetation changes: climate forcing and human impact. *Quaternary International* **200**: 4–18.
- Jombart T, Pontier D, Dufour AB. 2009.** Genetic markers in the playground of multivariate analysis. *Heredity* **102**: 330–341.
- Kaplan JO, Krumhardt KM, Ellis EC, Ruddiman WF, Lemmen C, Goldewijk KK. 2010.** Holocen carbon emissions as a result of anthropogenic land cover change. *Holocene Special Issue* **21**: 775–791.
- Keller I, Nentwig W, Largiadier CR. 2004.** Recent habitat fragmentation due to roads can lead to significant genetic differentiation in an abundant flightless ground beetle. *Molecular Ecology* **13**: 2983–2994.
- Klein Goldewijk K, Beusen A, van drecht G, de Vos M. 2010.** The HYDE 3.1 spatially explicit database of human-induced global land-use change over the past 12,000 years. *Global Ecology and Biogeography* **20**: 73–86.
- Krystufek B. 2010.** *Glis glis* (Rodentia: Gliridae). *Mammalian Species* **48**: 195–206.
- Kyle CJ, Strobeck C. 2001.** Genetic structure of North American wolverine (*Gulo gulo*) populations. *Molecular Ecology* **10**: 337–347.
- Langella O. 1999.** *Populations, Ver. 1.2.30. a population genetic software*. CNRS UPR9034. Available at: <http://bioinformatics.org/~tryphon/populations/>.
- Marquer L, Gaillard M-J, Sugita S, Poska A, Trondman A-K, Mazier F, Nielsen AB, Fyfe RM, Jönsson AM, Smith B, Kaplan JO, Alenius T, Birks HJB, Bjune AE, Christiansen J, Dodson J, Edwards KJ, Giesecke T, Herzschuh U, Kangur M, Koff T, Latałowa M, Lechterbeck J, Olofsson J, Seppä H. 2017.** Quantifying the effects of land use and climate on Holocene vegetation in Europe. *Quaternary Science Reviews* **171**: 20–37.
- Marteau M, Sarà M. 2015.** Habitat preferences of edible dormouse, *Glis glis italicus*: implications for the management of arboreal mammals in Mediterranean forests. *Folia Zoologica* **64**: 136–150.
- Martin PS. 2005.** *Twilight of the Mammoths: ice age extinctions and the rewilding of America*. Berkeley: University of California Press.
- Michaux JR, Goüy de Bellocq J, Morand S. 2002.** Body size increase in insular rodent populations: a role for predators? *Global Ecology and Biogeography* **11**: 427–436.
- Michaux JR, Libois R, Filippucci MG. 2005.** So close and so different: comparative phylogeography of two closely related rodent species (*Apodemus flavicollis* and *A. sylvaticus*) in the Western Palearctic region. *Heredity* **94**: 52–63.
- Michaux JR, Magnanou E, Paradis E, Nieberding C, Libois R. 2003.** Mitochondrial phylogeography of the Woodmouse (*Apodemus sylvaticus*) in the Western Palearctic region. *Molecular Ecology* **12**: 685–697.

- Michaux JR, Sara M, Libois RM, Matagne R. 1998. Is the woodmouse (*Apodemus sylvaticus*) of Sicily really a “separate” species? *Belgian Journal of Zoology* **128**: 211–214.
- Mondol S, Bruford MW, Ramakrishnan U. 2013. Demographic loss, genetic structure and the conservation implications for Indian tigers. *Proceedings of the Royal Society B* **280**: 20130496.
- Moreira F, Russo D. 2007. Modelling the impact of agricultural abandonment and wildfires on vertebrate diversity in Mediterranean Europe. *Landscape Ecology* **22**: 1461–1476.
- Morris P. 1997. A review of the fat dormouse (*Glis glis*) in Britain. *Natura Croatica* **6**: 163–176.
- Mortelliti A, Sanzo GS, Boitani L. 2008. Species’ surrogacy for conservation planning: caveats from comparing the response of three arboreal rodents to habitat loss and fragmentation. *Biodiversity and Conservation* **18**: 1131–1145.
- Mouton A, Krystufek B, Maurizio S, Randi E, Amori G, Rimvydas J, Grill A, Aloise G, Mortelliti A, Panchetti F, Michaux JR. 2012. Mitochondrial DNA reveals a complex phylogeographic structure of the common dormouse, *Muscardinus avellanarius* (Rodentia: Gliridae), in Europe. *Biological Journal of the Linnean Society* **105**: 648–664.
- Mouton A, Mortelliti A, Grill A, Sara M, Krystufek B, Juškaitis R, Latinne A, Amori G, Randi E, Büchner S, Schulz B, Ehlers S, Lang J, Adamik P, Verbeylen G, Dorenbosch M, Trout R, Elmeros M, Aloise G, Mazzoti S, Matur F, Poitevin F, Michaux JR. 2016. Evolutionary history and species delimitations: a case study of the hazel dormouse, *Muscardinus avellanarius*. *Conservation Genetics* **18**: 181–196.
- Naderi G, Kaboli M, Koren T, Karami M, Zupan S, Rezaei HR, Krystufek B. 2014. Mitochondrial evidence uncovers a refugium for the fat dormouse (*Glis glis* Linnaeus, 1766) in Hyrcanian forests of northern Iran. *Mammalian Biology* **79**: 202–207.
- Nei M. 1987. *Molecular evolutionary genetics*. New York: Columbia University Press.
- Nei M, Tajima F, Tateno Y. 1983. Accuracy of estimated phylogenetic trees from molecular data. II. Gene frequency data. *Journal of Molecular Evolution* **19**: 153–170.
- Nieberding C, Libois R, Morand S, Michaux JR. 2006. Parasites and the island syndrome: the colonisation of the Western Mediterranean islands by *Heligmosomoides polygyrus* (Dujardin, 1845). *Journal of Biogeography* **10**: 1365–1376.
- Olafsson K, Pampoulie C, Hjorleifsdottir S, Gudjonsson S, Hreggvidsson GO. 2014. Present-day genetic structure of Atlantic salmon (*Salmo salar*) in Icelandic rivers and ice-cap retreat models. *PLoS ONE* **9**: e86809.
- Petruso D, Sarà M, Surdi G, Masini F. 2011. Le faune a mammiferi della Sicilia tra il Tardoglaciale e l’Olocene. *Biogeography* **30**: 27–39.
- Pritchard JK, Stephens M, Donnelly P. 2000. Inference of population structure using multilocus genotype data. *Genetics* **155**: 945–959.
- Pritchard JK, Wen W. 2003. *Documentation for STRUCTURE software: Version 2*. Available at: <http://pritch.bsd.uchicago.edu>.
- Roberts N, Fyfe RM, Woodbridge J, Gaillard MJ, Davis BAS, Kaplan JO, Marquer L, Mazier F, Nielsen AB, Sugita S, Trondman AK, Leydet M. 2018. Europe’s lost forests: a pollen-based synthesis for the last 11,000 years. *Scientific Reports* **8**: 716.
- Roberts RG, Flannery TF, Ayliffe LK, Yoshida H, Olley JM, Prideaux GJ, Laslett GM, Baynes A, Smith MA, Jones R, Smith BL. 2001. New ages for the last Australian megafauna: continent-wide extinction about 46,000 years ago. *Science* **292**: 1888–1892.
- Rosenberg NA. 2004. DISTRUCT: a program for the graphical display of population structure. *Molecular Ecology Notes* **4**: 137–138.
- Rosenberg NA, Pritchard JK, Weber JL, Cann HM, Kidd KK, Zhivotovsky LA, Feldman MW. 2002. Genetic structure of human populations. *Science* **298**: 2381–2385.
- Ruddiman WF. 2003. The anthropogenic greenhouse era began thousands of years ago. *Climatic Change* **61**: 261–293.
- Ruddiman WF. 2007. The early anthropogenic hypothesis: challenges and responses. *Reviews of Geophysics* **45**: 1–37.
- Ruddiman WF. 2011. Can natural or anthropogenic explanations of late-Holocene CO₂ and CH₄ increases be falsified? *Holocene Special Issue* **21**: 865–879.
- Ruf T, Fietz J, Schlund W, Bieber C. 2006. High survival in poor years: life history tactics adapted to mast seeding in the edible dormouse. *Ecology* **87**: 372–381.
- Sabatini FM, Burrascano S, Keeton WS, Levers C, Lindner M, Pötzschner F, Verkerk PJ, Bauhus J, Buchwald E, Chaskovsky O, Debaive N, Horváth F, Garbarino M, Grigoriadis N, Lombardi F, Duarte IM, Meyer P, Midteng R, Mikac S, Mikoláš M, Motta R, Mozgeris G, Nunes L, Panayotov M, Ódor P, Ruete A, Simovski B, JStillhard J, Svoboda M, Szwagrzyk J, Tikkanen OP, Volosyanchuk R, Vrska T, Zlatanov T, Kuemmerle T. 2018. Where are Europe’s last primary forests? *Diversity and Distributions* **24**: 1426–1439.
- Saccheri I, Kuussaari M, Kankare M, Vikman P, Fortelius W, Hanski I. 1998. Inbreeding and extinction in a butterfly metapopulation. *Nature* **392**: 491–494.
- Scinski M, Borowski Z. 2008. Spatial organization of the fat dormouse (*Glis glis*) in an oak–hornbeam forest during the mating and post-mating season. *Mammalian Biology* **73**: 119–127.
- Simmons IG. 1996. *Changing the face of the earth*. Oxford: Blackwell.
- Sitzia T, Semenzato P, Trentanovi G. 2010. Natural reforestation is changing spatial patterns of rural mountain and hill landscapes: a global overview. *Forest Ecology and Management* **259**: 1354–1362.
- Sommer R, Nadachowski A. 2006. Glacial refugia of mammals in Europe: evidence from fossil records. *Mammal Review* **36**: 251–266.
- Stöck M, Sicilia A, Belfiore NM, Buckley D, Lo Brutto S, Lo Valvo M, Arculeo M. 2008. Post-Messinian evolutionary relationships across the Sicilian channel: mitochondrial and nuclear markers link a new green toad from Sicily to African relatives. *BMC Evolutionary Biology* **8**: 56.
- Sunnåker M, Busetto AG, Numminen E, Corander J, Foll M, Dessimoz C. 2013. Approximate Bayesian computation. *PLoS Computational Biology* **9**: e1002803.

- Taberlet P, Fumagalli L, Wust-Saucy AG, Cosson JF. 1998.** Comparative phylogeography and postglacial colonization routes in Europe. *Molecular Ecology* **7**: 453–464.
- Taberlet P, Griffin S, Goossens B, Questiau S, Manceau V, Escaravage N, Waits LP, Bouvet J. 1996.** Reliable genotyping of samples with very low DNA quantities using PCR. *Nucleic Acids Research* **24**: 3189–3194.
- Takezaki N, Nei M. 2008.** Empirical tests of the reliability of phylogenetic trees constructed with microsatellite DNA. *Genetics* **178**: 385–392.
- Thirgood JV. 1981.** *Man and the mediterranean forest*. London: Academic Press.
- Tresset A, Vigne JD. 2011.** Last hunter-gatherers and first farmers of Europe. *Comptes Rendus Biologies* **334**: 182–189.
- Van Oosterhout C, Hutchinson WF, Wills DPM, Shipley P. 2004.** Micro-checker: software for identifying and correcting genotyping errors in microsatellite data. *Molecular Ecology Notes* **4**: 535–538.
- Vigne JD, Valladas H. 1996.** Small mammal fossil assemblages as indicators of environmental change in Northern Corsica during the last 2500 years. *Journal of Archaeological Science* **23**: 199–215.
- Wang M, Schreiber A. 2001.** The impact of habitat fragmentation and social structure on the population genetics of roe deer (*Capreolus capreolus* L.) in Central Europe. *Heredity* **86**: 703–715.
- Weber K, Hoelzl F, Cornils J, Smith S, Biebera C, Balint B, Rufa T. 2018.** Multiple paternity in a population of free-living edible dormice (*Glis glis*). *Mammalian Biology* **93**: 45–50.
- Weir BS, Cockerham CC. 1984.** Estimating F-statistics for the analysis of population structure. *Evolution* **38**: 1358–1370.
- Zohary D, Hopf M. 1993.** *Domestication of plants in the old world*. Oxford: Oxford University Press.

SUPPORTING INFORMATION

Additional Supporting Information may be found in the online version of this article at the publisher's web-site.

Fig. S1. Seventeen evolutionary scenarios for the differentiation of European groups of edible dormice, tested using ABC analyses. The first three scenarios were based on the topology obtained by NJ analyses on (1) F_{st} values (Fig. 3A); (2) the D_a genetic distance index (Fig. 3B); and (3) the D_s genetic distance index (Fig. 3C). The fourth scenario was constructed according to the results obtained with the STRUCTURE software. The tree topology was created according to the progressive relationships among clusters from the hypothesis of $K = 2$ to $K = 12$. To explore possible space around these scenarios, 13 further scenarios, which make sense based on the biology of *Glis glis* and its phylogeographical history, were built by rearrangement of the branches in scenario 1. The names of populations correspond to those described in Figures 3–6.

Fig. S2. Results of PCA obtained with the diYABC software, showing the fit of the observed data (in yellow) to the simulated fit (light blue for prior and black circled blue for posterior Bayesian distributions).

Fig. S3. Graph representing the logistic regressions performed on 1% of the closest simulated datasets, distinguishing unambiguously the most likely of all tested scenarios at each step. The third scenario is the most likely, i.e. that based on the observed topology resulting from D_s distance values (Fig. 3C).

Table S1. Reference number, country abbreviation, inferred populations and number of edible dormouse specimens collected in the present study.

Table S2. Prior distributions of parameters used in our ABC analysis.

Table S3. Genetic distances between edible dormouse populations. Pairwise F_{st} values (Weir & Cockerham, 1984) calculated in ARLEQUIN are provided below the diagonal. Statistical significance of the difference is provided above the diagonal (***) $P < 0.00075$. N corresponds to the number of specimens per group.

Table S4. Performance analysis of the model choice procedure. D = proportion of cases in which the simulation-based model choice procedure selected a scenario as the most probable with non-overlapping confidence intervals of the posterior probabilities of each scenario. *Type-I or α -error rate. °Type-II or β -error rate ($1 - \sum \beta_i$ is used to determine the power of the model choice procedure).

Table S5. Posterior probabilities obtained for the most likely scenario (1) (see figure in Appendix 1). The effective sizes [from N_a (ancestral) to N_{12}] of each studied population as well the time split among them (from tC_1 to tC_9) are given. Confidence intervals (CI) (95%) are also given for each parameter.